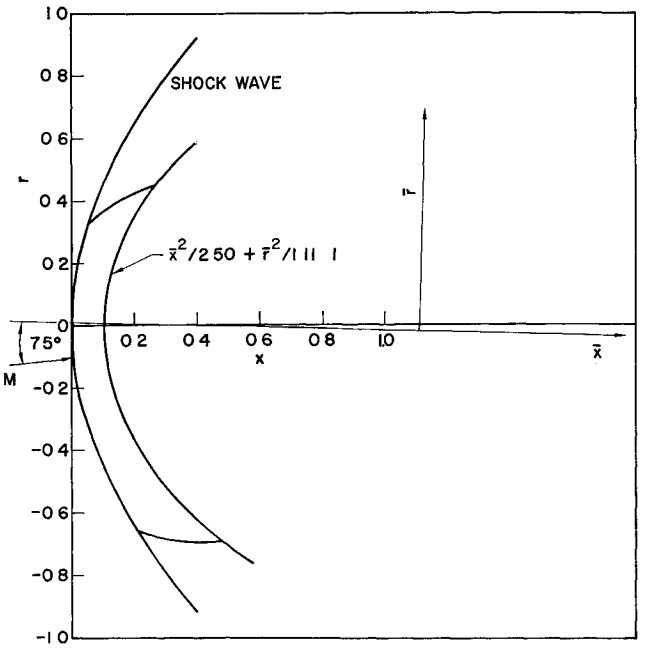

Fig 3 Body shape and sonic lines; 3:2 prolate ellipsoid of revolution, $M = 8.08$, $\gamma = 1.4$, $\epsilon = 6°$, $\alpha = 7.5°$

For a discussion of similar comparisons for flow past the body supporting a spherical shock at infinite freestream Mach number, and for flow past two-dimensional bodies supporting circular shock waves at freestream Mach numbers of infinity and 4.0, see Ref. 3. In general, body-shape agreement is good in the two-dimensional cases. Agreement of sonic-line positions and surface-pressure distributions, however, is only fair, being slightly poorer than the corresponding three-dimensional cases.

Figure 3 shows the profile in the vertical symmetry plane of a body having the same cross section in this plane as a 3-to-2 axis ratio prolate ellipsoid of revolution at 7.5° angle of attack. The body supports the shock wave shown at a freestream Mach number of 8.08. This Mach number was chosen in order that experimental results for the surface pressure distribution on a 3-to-2 prolate ellipsoid of revolution at 7.5° angle of attack could be compared with those of theory. The comparison is made in Fig. 4. Note that agreement between the theoretical curve and experimental data is excellent. In light of the previously discussed systematically high surface-pressure distributions predicted by theory, one must conclude that the error is small for this case (cf. Fig. 2). Note that the angle-of-attack of the body α is 7.5°. This corresponds to a shock-wave angle of attack ϵ of 6°. Hence, the reduction in ϵ^2 over the previously considered data is 64%, which aids significantly in reducing the error in the surface-pressure distribution.

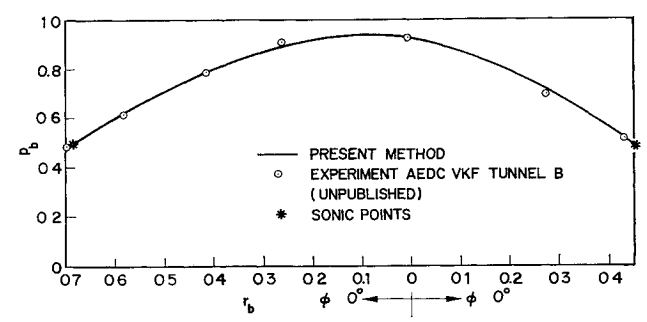

Fig 4 Surface pressure distribution; 3:2 prolate ellipsoid of revolution, $M = 8.08$, $\gamma = 1.4$, $\epsilon = 6°$, $\alpha = 7.5°$

References

[1] Swigart, R. J., "A theory of asymmetric hypersonic blunt-body flows," IAS Preprint 62-98 (June 1962).

[2] Vaglio-Laurin, R., "Inviscid supersonic flow about general three dimensional blunt bodies," TR ASD-TR-61-727, Vol. I, Flight Dynamics Lab., Aeronaut. Systems Div., Air Force Systems Command, Wright-Patterson Air Force Base, Ohio (October 1962).

[3] Swigart, R. J., "Hypersonic blunt body flow fields at angle of attack," Fluid Mech. Res. Rept. 5, Mech. and Math. Sci. Lab., Lockheed Missiles and Space Co., Palo Alto, Calif. (May 1963).

Determination of Propellant Properties by the Arc Image Furnace Technique

R. O. Fleming, Jr.* and R. W. Fleming†

Bermite Powder Company, Saugus, Calif.

THE arc image furnace technique[1] has been used for the past several years for the determination of threshold ignition energies (q) of propellants and igniter materials. The particular arc image design used in these studies consists of opposed ellipsoids with a shuttering mechanism at the common minor focus. A high intensity carbon arc located at the major focus of one ellipsoid is imaged on the sample surface located at the major focus of the other ellipsoid (see Fig. 1). The samples, which are about 8 mm in diameter by about 5 mm thick, are located precisely within a cylindrical cast acrylic firing chamber whose volume is about 125 cm³. The chamber can be subjected to varying environmental conditions of pressure, temperature, and flow.

An Elastronics, Inc.,‡ type TR 4001 radiation transducer is located at one end of the firing chamber so that it views the sample surface to be irradiated. The transducer consists of a germanium photo transistor located behind a sapphire "light pipe" and is capable of producing temperature vs time profiles by means of an oscilloscope and recording camera.

In practice, the firing chamber is connected to a surge tank whose volume is about 12,500 cm³. The material to be tested is either cut (in the case of the solid propellants) or press-loaded in suitable retaining rings (in the case of igniter materials). Sample thickness is determined micrometrically. The rear surface of each sample is spotted with a drop of bead mix which contains a high percentage of zirconium. Each sample is then exposed to a predetermined amount of energy and "go/no-go" data is obtained so that the Bruceton or

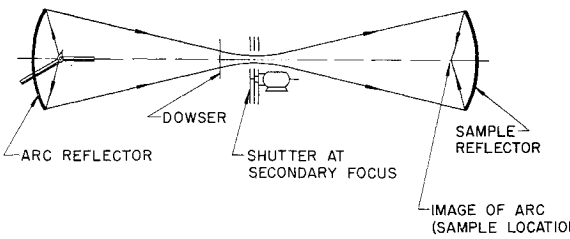

Fig 1 Schematic drawing of double ellipsoidal mirror system

Received September 18, 1963. The work described in this technical note was supported by the U. S. Navy, Bureau of Weapons, Contract NOw 62-0236-c.

* Manager, Research Group, Research and Development Division.

† Engineer, Research Group, Research and Development Division.

‡ Elastronics Inc., 19458 Ventura Blvd., Tarzana, Calif.

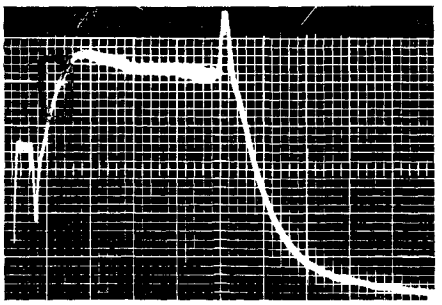

Fig 2 Temperature vs time profile of metal-oxidant mix at 250-psig environmental pressure

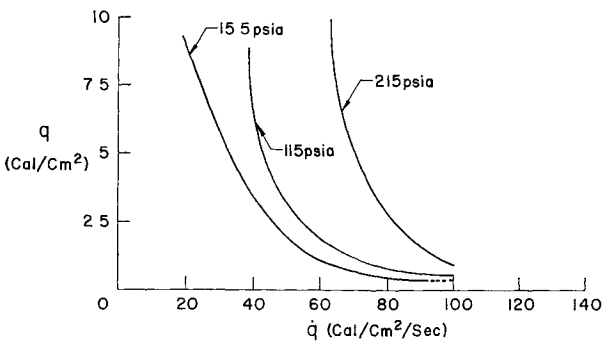

Fig 3 Approximate relationships of threshold ignition energy to flux at three pressure levels for a metal-oxidant mix at a consolidation pressure of 46,000 psi

"up-down" method[2] of statistical analysis can be employed to yield the q value estimate of the mean Since the shuttering mechanism delivers the energy in essentially a square wave form, the following relationship applies:

$$q = \dot{q}t \tag{1}$$

where $\dot{q}$ is the flux or rate at which the energy is delivered and t is the time The $\dot{q}$ range can be varied from about 15 to 125 cal/cm²/sec, and the shuttering arrangement permits continuously variable, predetermined time increments between 5 and 2000 msec Calibration is obtained by means of a copper-constantan calorimeter

Samples ignited during a given analytical run are recorded by the radiation transducer previously described The ignition point with respect to time is clearly visible on the oscilloscope traces When the burning wave front reaches the end of the sample, the zirconium bead mix is ignited, thus producing an intense signature (see Fig 2) The burning time can then be measured, and since the sample length is known, the burning rate is easily determined Burning rate exponents obtained in this manner indicate close agreement with those obtained by the Crawford strand-burner method [3]

Since the $\dot{q}$ can be varied by the introduction of steel wire mesh screens near the shuttering mechanism, the manner in which the q value of a particular material varies with $\dot{q}$ can be easily ascertained [4] Figure 3 shows the q vs $\dot{q}$ relationship of a metal-oxidant mix at three environmental pressure levels

References

[1] Null, M R and Lozier, W W, "Carbon arc image furnaces," Rev Sci Instr 29, 163–170 (1958)

[2] Crow, E L, Davis, F A, and Maxfield, M W, *Statistics Manual* (Dover Publications, Inc New York, 1960), 1st ed, Chap IV

[3] Crawford, B L, Huggett, C, Daniels, F, and Wilfong, R E, "Direct determination and burning rates of propellant powders," Anal Chem 19, 630–633 (1947)

[4] Price, E W, Bradley, H H, Jr, and Fleming, R O, Jr, "Ignition of solid propellants," Spring Meeting of the Combustion Institute, San Diego, Calif (1963)

Phase Shift in a Massless Vibrating Beam

JOSEPH GENIN*
General Dynamics, Fort Worth, Texas

THIS note is a simple demonstration of a phase shift in a massless vibrating beam The mathematical model shown in Fig 1 consists of a massless cantilever beam with a concentrated mass at its free end being driven by a forcing function $F_0e^{i\omega t}$

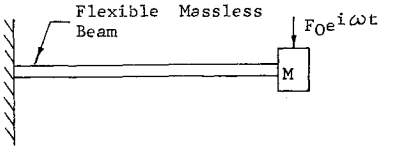

Fig 1 Mathematical model for the study of the phase shift

A free-body diagram in which the beam is represented as a series of elastic and viscous elements is shown in Fig 2 In general, the equation of motion for any section is

$$M\ddot{x}_n = -k_j(x_j - x_{j-1}) - c_j(\dot{x}_j - \dot{x}_{j-1}) + F_0e^{i\omega t} \tag{1}$$

where j represents the section being considered Consider the steady-state solution to Eq (1):

$$x_j = A_je^{i\omega t} \tag{2}$$

where the A_j are complex Values for A_j may be obtained

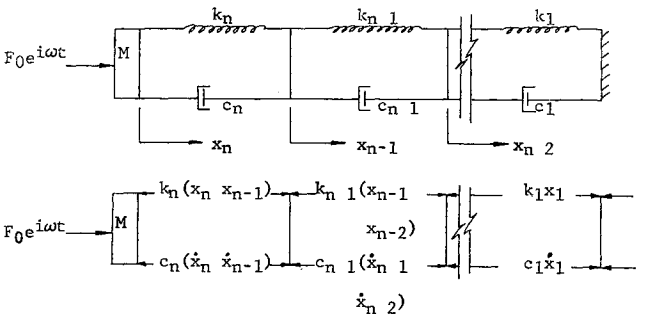

Fig 2 Free-body diagram of the mathematical model

by placing Eqs (2) into Eqs (1) Letting $A_j = r_je^{i\alpha_j}$, a ratio of successive amplitudes is found to be

$$\frac{A_j}{A_{j-1}} = \frac{r_j}{r_{j-1}}\, e^{i(\alpha_j - \alpha_{j-1})} \tag{3}$$

Using Eqs (1–3), the phase shift at any position along the beam may be formulated Hence, an arbitrary selection of $n = 3$ and $j = 2$ yields,

$$\tan(\alpha_2 - \alpha_1) = \frac{(c_1k_2 - c_2k_1)\omega}{k_2(k_1 + k_2) + \omega^2c_2(c_2 + c_1)} \tag{4}$$

For $c_1 = c_2$ and $k_1 = k_2$, Eq (4) reduces to $\tan(\alpha_2 - \alpha_1) = 0$, which implies that no phase difference exists between the different massless sections Physically, this represents a uniform beam where the damping is not a function of displace-

Received September 16, 1963; revision received October 10, 1963

* Senior Structure Engineer